

## Analysing the potential of *Nephelium lappaceum* L. peel as an anti-lung cancer agent through an *in-silico* study

Muhammad Farid<sup>1\*</sup>, Rachma Greta Perdana Putri<sup>1</sup> and Dwi Utami<sup>2</sup>

<sup>1</sup>Department of Medicine, Faculty of Medicine, Ahmad Dahlan University, Yogyakarta 55166, Indonesia

<sup>2</sup>Department of Analytical and Medicinal Chemistry, Faculty of Pharmacy, Ahmad Dahlan University, Yogyakarta, 55164, Indonesia

Received 06 March 2025; revised received 10 October 2025; accepted 30 October 2025

Lung cancer has a high mortality rate, especially in Indonesia. The use of conventional drugs often causes side effects, so alternatives are needed. Rambutan peel, rich in flavonoids and phenols, has potential as an anticancer agent. This research aims to evaluate the potential of rambutan peel as an anti-lung cancer agent using an *in-silico* approach. The study was conducted using pharmacokinetic predictions from SwissADME to ensure the suitability of oral drug parameters. Network pharmacology analysis to map interactions between active compounds in rambutan peel and proteins associated with lung cancer. Molecular docking was carried out to determine the interaction of the test ligand with the target protein using Autodock, with the binding visualisation results analysed using Biovia software. The results of this study show that of the 11 compounds, five are active compounds that comply with the Lipinski rules. Out of the five compounds studied, 84 protein targets were found, with SRC and EGFR showing the most interactions. From these, 21 proteins were linked to the KEGG pathway related to lung cancer, and based on GO and KEGG analysis, the main pathway identified was EGFR tyrosine kinase inhibitor resistance. The apigenin compound has the highest potential as an anti-lung cancer agent through EGFR inhibition with a binding energy value of -6.65 kcal/mol. The dominant interacting amino acids across all ligands are ASP323, SER324, and ASN331 for hydrogen bonds, and ARG42 and LEU325 for non-hydrogen interactions. This research concludes these findings suggest a potential inhibitory effect, warranting further experimental validation.

**Keyword:** *In-silico*, Lung cancer, *Nephelium lappaceum*, Phytochemical compounds

**IPC code; Int. cl. (2021.01)**–A61K 36/00, A61K 131/00, A61P 35/00

### Introduction

Cancer or malignancy is a disease that has a poor prognosis, with the incidence always increasing every year. Global Cancer Statistics 2023 shows that lung cancer is ranked 2nd with a high death rate of 127,070 cases per year<sup>1</sup>. Lung cancer in Indonesia ranks third after breast cancer and cervical cancer<sup>2</sup>. Exposure to cigarettes increases the risk of lung cancer by 25%<sup>3</sup>. Gene mutations play an important role in the expression of oncogenic traits, with loss of the ability of cancer cell suppressor genes to provide opportunities for cell proliferation<sup>4</sup>. The PI3K, AKAT1, PTEN, and mTOR pathways have important regulations in the development of cancer cells and these genes are targets for lung cancer treatment<sup>5</sup>. Jonna S *et al.*, shows the effectiveness of oral anti-lung cancer drugs such as vepesid, hycamtin, temodar, navelbine, tetsuno, and xeloda in suppressing the development of oncogene cells. These drugs have side effects in the form of haematological diseases such

as anaemia, neutropenia and asthenia, so that other alternatives are needed for treatment<sup>6</sup>.

The use of natural ingredients in herbal medicine offers a promising alternative to conventional chemical treatments. One such potential source is the rambutan plant (*Nephelium lappaceum* L.), an endemic species in Indonesia, which has long been utilised in traditional medicine<sup>7</sup>. Rambutan peel, in particular, has been used for generations to treat ailments such as dysentery, and is known for its antimicrobial and anti-diabetic properties<sup>8</sup>. Studies have shown that methanol extracts of rambutan peel contain bioactive compounds including flavonoids, coumarins, and phenols, which exhibit anti-proliferative effects on human oral carcinoma cells<sup>9</sup>. While certain flavonoids, such as apigenin, have been well-researched for their anticancer potential, their presence in *N. lappaceum* peel and their interactions with proteins related to lung cancer remain underexplored<sup>10</sup>. Given that rambutan peel is often discarded as agricultural waste, particularly during peak harvest seasons, it poses an environmental concern<sup>11</sup>. This abundance, however, presents an opportunity to develop standardised herbal

\*Correspondent author  
Email: muhammad2100034023@webmail.uad.ac.id

medicines by harnessing the peel's rich bioactive content.

*In silico* studies are preliminary tests for drug development that utilise computational bioinformatics methods to investigate molecular interactions between proteins and test compounds<sup>12</sup>. Prediction of absorption, distribution, metabolism, excretion and toxicity (ADMET) is used as the most important screening method to determine the kinetic mechanism of a compound in the body<sup>13</sup>. Networking pharmacology or pharmacological networking is carried out to determine complex pharmacological processes between compounds through biological pathways<sup>14</sup>. Molecular docking is the process of docking a compound as a test ligand against a target protein using computational-based methods<sup>15</sup>. This study is an important aspect for developing new drugs that study at the level of small molecules, such as amino acids and atoms<sup>16</sup>. Based on the background mentioned above, researchers are interested in conducting *in silico* tests on the active compounds of rambutan peel as anti-lung cancer agents. It is hoped that this study can provide concrete information regarding the predicted ability of rambutan peel as an anti-lung cancer agent.

## Method

This research utilised computational methods to explore the potential anticancer effects of active compounds from rambutan peel (*N. lappaceum* L.) by investigating their interactions with proteins related to lung cancer.

### Pharmacokinetic profile prediction

Active compounds were analysed using SwissADME to predict physicochemical and pharmacokinetic properties via their Canonical SMILES input. The results are then reconstructed using a new table containing components that correspond to the required oral drug parameters. Compounds were filtered based on Lipinski's rule of five and additional criteria, including molecular weight (<500 g/mol), hydrogen bond donors (<5), acceptors (<10), LogP (<5)<sup>17</sup>, molar refractivity (62.17–131.57 cm<sup>3</sup>/mol), and topological polar surface area (20–130 Å<sup>2</sup>)<sup>18</sup>.

### Network pharmacology

The selected active compounds underwent target prediction using the Superpred platform, which estimates potential protein targets based on chemical similarity and bioactivity data. Concurrently, lung cancer-related protein targets were retrieved from the GeneCards database and filtered by relevance score to

ensure high-confidence targets. Overlapping proteins between compound targets and lung cancer-associated proteins were identified via Venny 2.1 to pinpoint potential therapeutic targets. These intersecting proteins were further analysed for their interactions through the STRING database to build a protein-protein interaction (PPI) network.

This network was visualised using Cytoscape software, which allows mapping proteins and interactions. Using Cytohubba, key hub proteins within the network were identified based on connectivity and centrality measures, highlighting proteins most likely involved in disease progression and compound action. To understand the biological context, pathway enrichment analysis was conducted using KEGG to determine which signalling pathways these hub proteins are involved in, with an emphasis on those related to lung cancer mechanisms.

### Molecular docking

Protein structures selected from network pharmacology were obtained from the Protein Data Bank (PDB). Before docking, these structures were prepared by removing non-essential molecules such as native ligands, water, and cofactors using Biovia Discovery Studio 2021 to ensure accurate simulation of ligand binding. Docking protocol validation was performed by re-docking the native ligand to confirm the method's reliability, with an RMSD cutoff below 3 Å considered acceptable for reproducibility using AutoDock 1.5.7<sup>19</sup>.

The docking grid was defined based on the native ligand's binding pocket coordinates, ensuring focus on the biologically relevant site. Test compounds were docked to the prepared protein targets using AutoDock 1.5.7, generating binding affinity scores ( $\Delta G$ ) and inhibition constants ( $K_i$ )<sup>19</sup>. Results were benchmarked against native ligands and standard control drugs to evaluate relative binding strengths. The interactions between ligands and amino acid residues within the binding site were visualised with Biovia, highlighting hydrogen bonds, hydrophobic contacts, and other interactions crucial for binding stability. This step elucidates the molecular basis by which active compounds may inhibit target proteins involved in lung cancer.

The selected receptor structure (1MOX), representing a human-derived protein without crystallisation engineering, was refined and validated through re-docking of its native ligand to assess the reliability of the docking protocol. The process yielded a Root Mean

Square Deviation (RMSD) of 2.57 Å, which falls within the generally accepted threshold of <3 Å, indicating good reproducibility<sup>19</sup>. However, given its proximity to the upper limit, this result should be interpreted with caution, despite similar values being accepted in previous studies. To ensure accurate targeting of the biologically active site during docking, the grid box was defined based on the native ligand's binding pocket, with the following parameters: centre coordinates at X: -38.217, Y: 83.863, Z: 26.053; number of grid points set to 40 × 40 × 40; and grid spacing of 0.375 Å.

## Results and Discussion

### Pharmacokinetic profile prediction

Prediction of the physical and chemical properties of the active compounds of rambutan peel using the website Swiss ADME by entering Canonical SMILES. The results of drug similarity analysis using the swisADME website with Lipinski rule parameters (Table 1). The results of the analysis of the similarity of compounds to drugs using the Lipinski rule showed that there were five compounds that had suitable results. These five compounds are apigenin, pelargonidin, brevifolin carboxylic acid, ellagic acid, and p-coumaroyl glucose. These compounds will enter the next stage of research. Other compounds have HBA and HBD values that exceed the limit, namely those with an MW of >500 g/mol, except for Ellagic acid and pentoside, which have an MW of 434.31. The control drugs etoposide and vinorelbine had MW and HBA that exceeded Lipinski's rule limits, indicating poor physicochemical properties. The results of this analysis show that there are differences in the solubility of compounds in the body, which can affect their effectiveness.

### Network pharmacology

The exploration of bioactive compounds from rambutan peel (*Nephelium lappaceum* L.) through a network pharmacology approach provides a deeper understanding of their potential anticancer activity, particularly against lung cancer<sup>20</sup>. In this study, compounds that complied with Lipinski's Rule of Five used to predict drug-likeness were selected for further analysis. These selected compounds were subjected to bioinformatics screening to predict their general biological targets using the SuperPred web server. The resulting protein targets were then further examined through STRING database analysis to establish the interaction network.

To identify proteins relevant to lung cancer, a comprehensive list was obtained from the GeneCards database using the keyword "lung cancer." The overlapping proteins between the predicted compound targets and the lung cancer-associated proteins were identified using Venny 2.1 (Fig. 1), resulting in 84 overlapping proteins out of 85 predicted targets, with one target (KDM4E) not intersecting with the cancer-related protein dataset. The protein-protein interaction (PPI) network constructed from these overlapping proteins consisted of 84 nodes and 291 edges, demonstrating significant interaction enrichment with a p-value of less than 1.0e-16, indicating a high level of biological connectivity. Among the identified pathways, the MAPK signalling pathway emerged as the most involved, featuring 14 of the mapped proteins, suggesting a potentially critical role in mediating the biological effects of the compounds on lung cancer progression.

The result of the analysis of protein-protein interactions resulting from all intersections of cancer compounds and proteins (Fig. 2). Pathway analysis

Table 1 — Lipinski analysis results

Molecules	MW	HBA	HBD	MR	TPSA	MLOGP	Lipinski
Apigenin	270.24	5	3	73.99	90.90	0.52	+
Pelargonidin	271.24	5	4	74.15	94.06	0.86	+
Brevifolin carboxylic acid	292.20	8	4	68.18	145.27	-0.70	+
Ellagic acid	302.19	8	4	75.31	141.34	0.14	+
p-Coumaroyl glucose	326.30	8	5	77.11	136.68	-1.12	+
Ellagic acid pentoside	434.31	12	6	101.46	200.26	-1.30	-2
Vitisin A	906.93	12	10	255.47	220.76	3.78	-3
Corilagin	634.45	18	11	141.85	310.66	-2.42	-3
Castalagin	934.63	26	16	211.49	455.18	-3.23	-3
Casuarinin	936.65	26	16	212.50	455.18	-3.23	-3
Geraniin	952.64	27	14	208.10	450.25	-3.45	-3
Etoposide	588.56	13	3	139.11	160.83	-0.14	-2
Vinorelbine	778.93	10	2	226.04	133.87	2.87	-2

results that correspond to the lung cancer process are available in the KEGG online database (DBGET Search Result: KEGG lung cancer). GO analysis results (Fig. 3) and KEGG Pathway of core proteins are shown below (Fig. 4). The results of pathway analysis showed that 21 target proteins had activity on lung cancer coding proteins. GO analysis of these

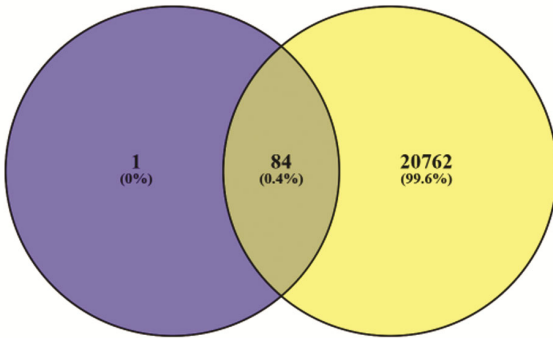


Fig. 1 — Intersection between compound target proteins and lung cancer coding proteins.

21 proteins shows the molecular activity of each protein, as shown in Fig. 3. GO analysis has three important aspects in the activity of a protein, namely biological process (BP), molecular function (MF), and cellular component (CC)<sup>21</sup>. BP analysis shows molecular activity together with MF. The results of the analysis revealed four biological process with full activity, namely 21 activities. MF analysis is gene activity at the molecular level, the highest analysis results are in the protein binding category with full activity, namely 21 activities. CC analysis as the activation location of each protein, the results show nucleus and membrane as the highest categories, with 15 activities.

KEGG analysis refers to molecular activity databases as knowledge in functional orthology mapping that connects various biological activity systems. The enrichment analysis carried out in Fig. 4 shows that EGFR tyrosine kinase inhibitor resistance has the highest value, with a value of 35.021. The enrichment results show that the pathways that are

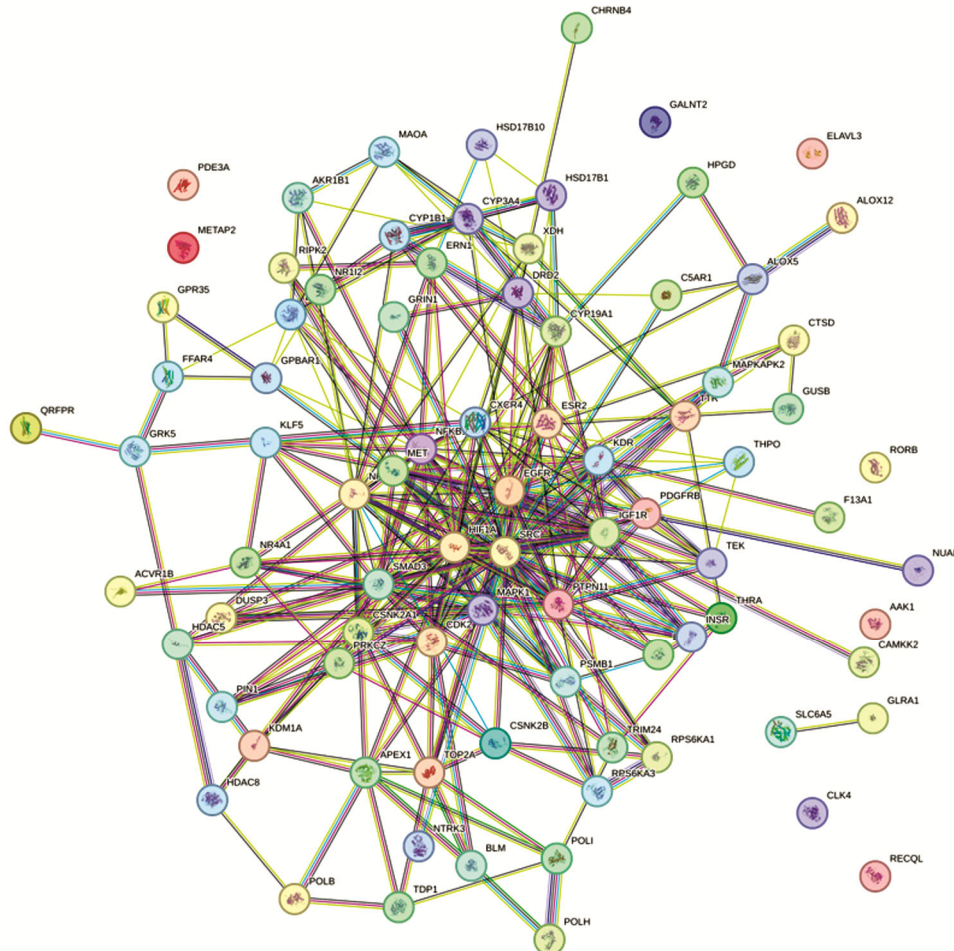


Fig. 2 — Results of specific protein-protein interactions.

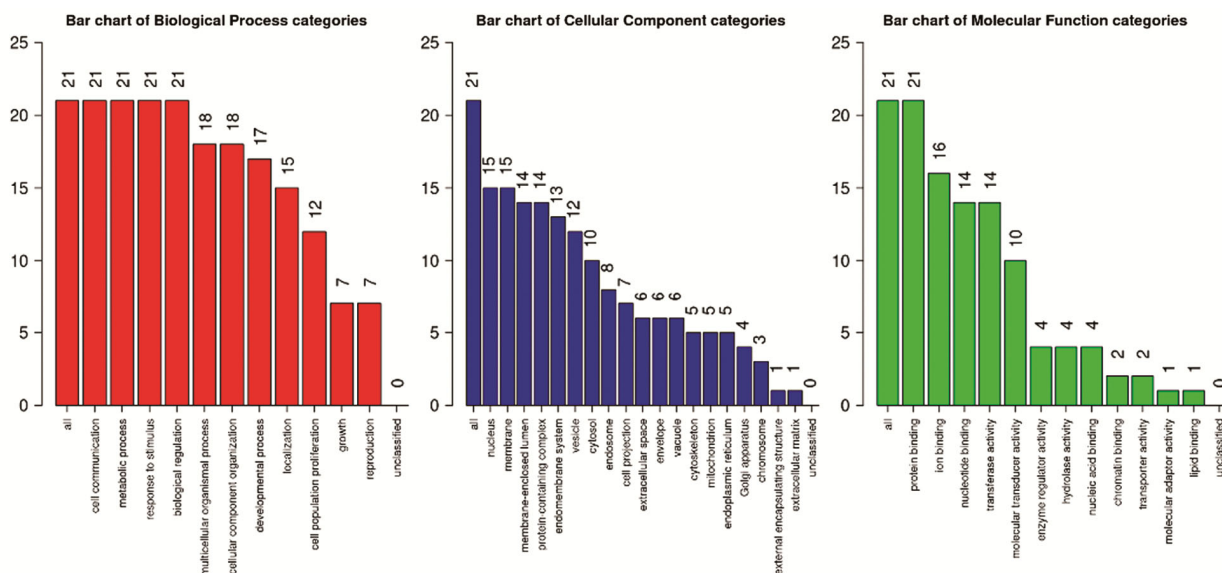


Fig. 3 — GO Analysis Results.

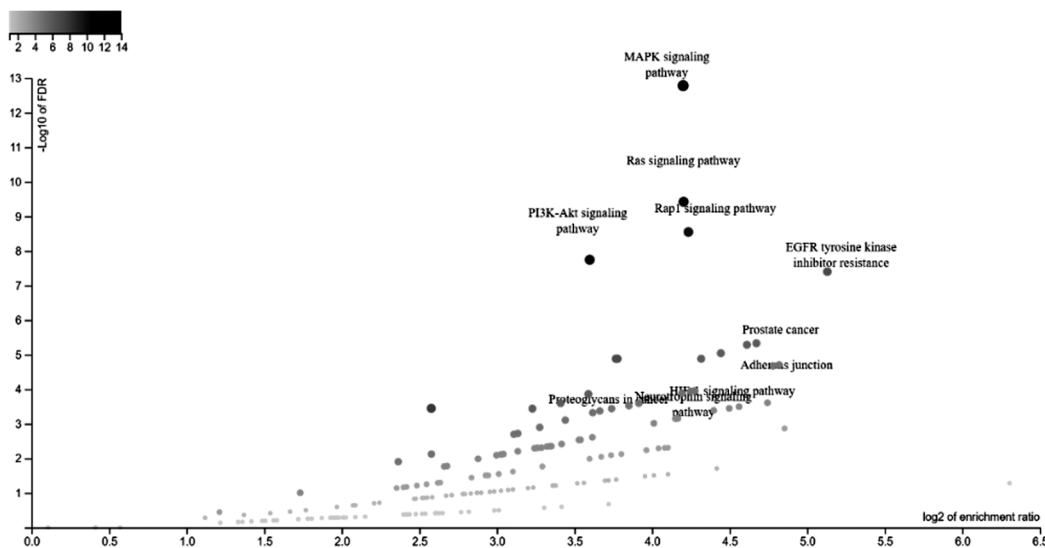


Fig. 4 — KEGG analysis results.

related to lung cancer are the Ras signalling pathway, the MAPK signalling pathway, and PI3K-Akt signalling pathway. The results of this analysis show the magnitude of the pathways associated with lung cancer in 21 target proteins.

The result of visualisation of the activity interaction between rambutan peel and lung cancer proteins using software Cytoscape by placing each component into a node or edge (Fig. 5) Visualisation of the compound-target-pathway network was performed using Cytoscape, which provided a comprehensive map of interactions involving botanical sources (represented as dark green circles), active compounds (light green

circles), biological pathways (light blue hexagons), core proteins (dark red diamonds), and specific cancer-related proteins (orange triangles). Analysis PPI of core proteins that correspond to pathways using cytohubba to obtain 10 proteins with the highest interactions as targets in molecular docking analysis (Fig. 6).

The results of the findings of the protein with the highest interaction at bland 8 show that SRC has the highest value, namely 15, followed by the EGFR and PTPN11 proteins with the same interaction value, namely 14. Inhibition of SRC can reduce stimulation of fibroblasts in cancer (CAF), angiogenesis and immune cell infiltration<sup>22,23</sup>. NSCLC patients using



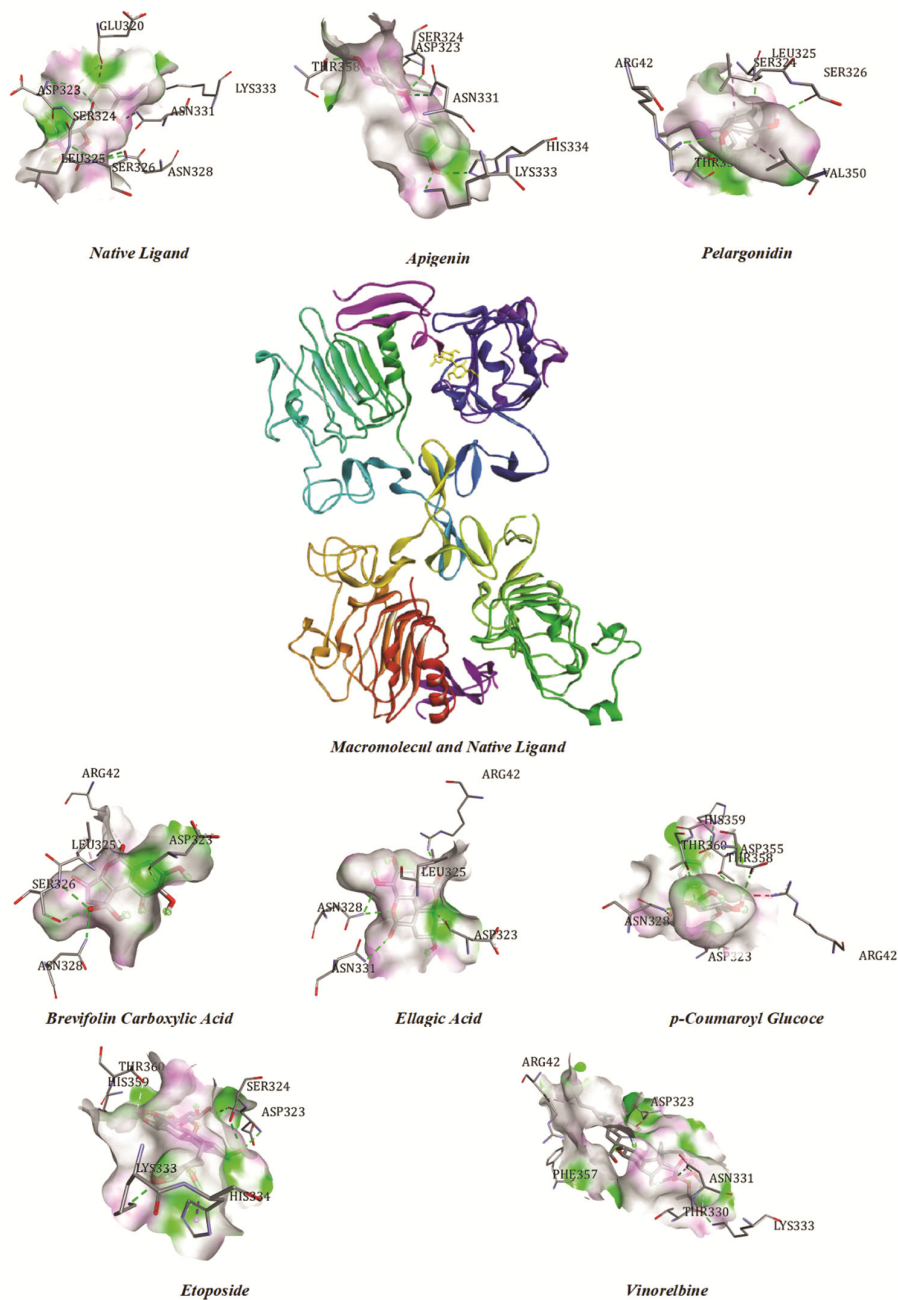


Fig. 7 — EGFR protein (PDB ID: MOX) and receptor after repair.

Table 2 — Grid box analysis results in the redocking process

Coordinates of Grid Points			Number of Grid Points			Spacing of Grid Points	RMSD
X	Y	Z	X	Y	Z	0.375 Å	2.57
-38,217	83,863	26,053	40	40	40		

**Molecular docking**

Molecular docking analysis was conducted using the 1MOX protein structure, chosen for its close representation of a human protein relevant to the study. Before docking, the protein and ligands underwent

thorough preparation to ensure optimal conditions for simulation (Fig. 7). Ligands, including both active compounds and control drugs, were geometrically optimised and energy-minimised to achieve stable conformations that closely resemble their natural

Table 3 — Results of molecular docking analysis of rambutan peel compounds and control drugs against IMOX

Compound	Binding Energy	Amino Acid Residues	
		Hydrogen	Non-Hydrogen
Native ligands	-6.65 kcal/mol	SER <sup>324,326</sup> , ASN <sup>328,331</sup> , ASP <sup>323</sup> , LEU <sup>325</sup> , GLU <sup>320</sup> , LYS <sup>333</sup>	GLU <sup>320</sup>
Apigenin	-6.65 kcal/mol	HIS <sup>334</sup> , SER <sup>324</sup> , ASP <sup>323</sup> , THR <sup>358</sup> , ASN <sup>331</sup> , LYS <sup>333</sup>	-
Pelargonidin	-5.75 kcal/mol	SER <sup>326, 324</sup> , ARG <sup>42</sup> , THR <sup>358</sup> ,	LEU <sup>325</sup> , VAL <sup>350</sup>
Brevifolin carboxylic acid	-6.05 kcal/mol	ASN <sup>328</sup> , SER <sup>326</sup> , ARG <sup>42</sup> , ASP <sup>323</sup>	LEU <sup>325</sup>
Ellagic acid	-5.70 kcal/mol	ASN <sup>328,331</sup> , ARG <sup>42</sup> , ASP <sup>323</sup>	LEU <sup>325</sup>
p-Coumaroyl glucose	-4.35 kcal/mol	THR <sup>360,358</sup> , ASP <sup>355,323</sup> , HIS <sup>359</sup> , ASN <sup>328</sup>	ARG <sup>42</sup>
Etoposide	-6.86 kcal/mol	LYS <sup>333</sup> , SER <sup>324</sup> , ASP <sup>323</sup> , THR <sup>359</sup> , HIS <sup>334</sup>	HIS <sup>359</sup>
Vinorelbine	-6.62 kcal/mol	LYS <sup>333</sup> , ASN <sup>331</sup> , THR <sup>330</sup> , ASP <sup>323</sup> , PHE <sup>357</sup>	ARG <sup>42</sup> , ASP <sup>323</sup>

biological states. The docking protocol was carefully validated through re-docking of the native ligand, producing an RMSD value of 2.57 Å, which confirms the method's reliability within the accepted accuracy range. This validation step ensures that the docking simulations provide trustworthy predictions of ligand-receptor interactions. The docking grid was precisely defined based on the native ligand's binding pocket, focusing the simulation on the most relevant active site (Table 3).

Molecular docking analysis in this study was based on the lowest binding free energy ( $\Delta G$ ) values obtained for each ligand-receptor complex, as summarised in Table 3. Among all tested compounds, etoposide, used as a positive control, demonstrated the most favourable binding affinity, with a  $\Delta G$  value of -6.86 kcal/mol. Apigenin followed closely with a binding energy of -6.65 kcal/mol, a value comparable to that of the native ligand. Although apigenin ranked second, the slight difference in energy compared to etoposide raises questions regarding its clinical significance, as minor variations in docking scores may not necessarily correspond to significant differences in biological activity or therapeutic efficacy. Another control drug, vinorelbine, showed a binding energy of -6.62 kcal/mol, identical to that of brevifolin carboxylic acid.

Meanwhile, pelargonidin and ellagic acid demonstrated moderate binding affinities at -5.75 and -5.70 kcal/mol, respectively. The weakest interaction was observed in p-coumaroyl glucose, which recorded a binding energy of -4.35 kcal/mol. While these  $\Delta G$  values offer useful insight into the potential of each compound to interact with the receptor, it is essential to interpret them cautiously. Computational predictions alone cannot fully capture the complexity of biological interactions, and small differences in binding energy should ideally be supported by *in vitro* or *in vivo* validation to confirm pharmacological relevance.

Visualisation of the ligand-receptor complexes at the binding pocket (Fig. 8) revealed specific amino acid

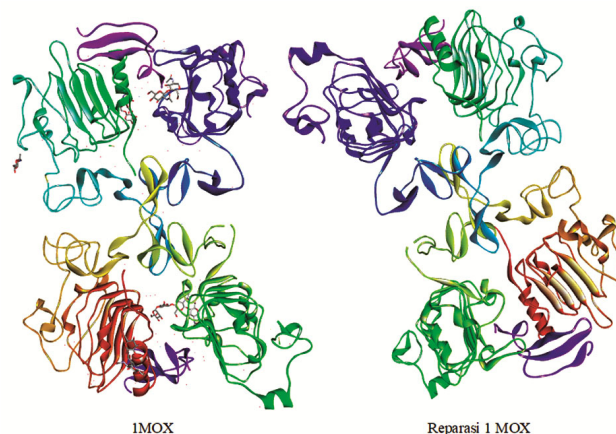


Fig. 8 — Best pocket pose from docking results.

interactions for each ligand. These interactions are driven by structural adjustments during docking, where favourable conformational alignments and electrostatic interactions stabilise the ligand within the receptor's active site. For apigenin, the docking results indicated the formation of multiple hydrogen bonds with key amino acid residues, including HIS334, SER324, ASP323, THR358, ASN331, and LYS333, suggesting strong and specific binding at the receptor interface.

Further analysis of amino acid interactions (Table 3) showed distinct patterns among other ligands. Pelargonidin formed hydrogen bonds with SER326, SER324, ARG42, and THR358, along with hydrophobic (alkyl) interactions involving LEU325 and VAL350. Brevifolin carboxylic acid exhibited hydrogen bonding with ASN328, SER326, ARG42, and ASP323, and hydrophobic contacts with LEU325. Similarly, ellagic acid established hydrogen bonds with ASN328, ASN331, ARG42, and ASP323, and displayed alkyl interactions with LEU325. Across all ligand-receptor complexes, several amino acids were consistently involved in binding. ASP323, SER324, and ASN331 emerged as the most frequent participants in hydrogen bonding, indicating their pivotal roles in ligand

stabilization<sup>31</sup>. For non-polar interactions, ARG42 and LEU325 were recurrent, suggesting that they contribute significantly to the hydrophobic stabilisation of ligand-receptor complexes. These findings highlight the importance of both hydrogen bonding and hydrophobic interactions in mediating and maintaining the affinity of bioactive compounds within the receptor binding site.

The findings of this study suggest that compounds derived from rambutan peel hold potential as anti-lung cancer agents, primarily through the inhibition of EGFR-related pathways. This aligns with earlier studies that have reported the anti-proliferative activity of rambutan peel extracts against various cancer cell lines, including MDA-MB-231 targeting breast cancer and MG-63 targeting osteosarcoma, where notable cytotoxic effects were observed<sup>32</sup>. Similar pro-apoptotic activity has also been demonstrated in HepG2 liver cancer cells, marked by DNA fragmentation and apoptotic induction<sup>9</sup>. Among the identified bioactive compounds, apigenin emerged as the most promising candidate due to its documented ability to inhibit cell proliferation, invasion, and migration, along with its capacity to induce apoptosis. Previous research has also confirmed apigenin's anti-lung cancer activity via suppression of GLUT1 expression and downregulation of the PI3K/AKT signalling pathway<sup>33,34</sup>.

Despite these encouraging results, direct comparisons with established EGFR inhibitors indicate that although phytochemicals such as apigenin may share similar interaction profiles, they typically exhibit weaker binding affinities. This suggests potential for synergistic or adjunctive use, but also underscores the need for more definitive comparative studies. The integration of network pharmacology and molecular docking in this study represents a novel approach to identifying therapeutic targets and mechanisms for rambutan-derived compounds. However, the findings remain preliminary, as the study relies exclusively on *in silico* methodologies, including docking simulations, pathway enrichment analyses, and target predictions from publicly available bioinformatics databases.

While these computational techniques are valuable for hypothesis generation and mechanism exploration, they cannot substitute for experimental validation. The lack of supporting *in vitro* or *in vivo* data, such as cell viability assays, apoptosis detection, or animal model studies, limits the translational significance of these results. Therefore, to advance these findings toward therapeutic application, further experimental studies are essential to confirm the biological activity, efficacy, and safety of the identified compounds.

## Conclusion

Five phytochemical compounds that met Lipinski's rule were selected for further analysis. Out of 85 identified targets, 84 showed alignment with proteins associated with lung cancer. Gene ontology results indicated strong associations with protein binding functions and nuclear localisation, while KEGG pathway mapping highlighted the involvement of EGFR tyrosine kinase inhibitor resistance in cancer progression. Core proteins such as SRC, EGFR, and PTPN11 were found to play significant roles in the interaction network. EGFR, in particular, was chosen for docking due to its established role in lung cancer biology and availability in a non-engineered crystal structure (1MOX). Docking validation produced an RMSD of 2.57 Å, which falls within the acceptable range for structural alignment. Apigenin demonstrated a binding energy of -6.65 kcal/mol and interacted with several key residues, including HIS334 and ASP323. However, this binding energy remains slightly less favourable than that of standard treatments such as etoposide (-6.86 kcal/mol), indicating that the phytochemicals may not surpass current drug standards. As no experimental data have been included, these findings remain predictive in nature and require biological assays to confirm actual inhibitory effects on cancer-related proteins.

## Acknowledgment

All authors declare that they have no potential conflicts of interest.

## References

- 1 Siegel R L, Miller K D, Wagle N S and Jemal A, Cancer statistics 2023, *CA Cancer J Clin*, 2023, **73**(1), 17–48, doi: 10.3322/caac.21763.
- 2 Asmara O D, Tenda E D, Singh G, Pitoyo C W, Rumende C M, *et al.*, Lung Cancer in Indonesia, *J Thorac Oncol*, 2023, **18**(9), 1134–1145, doi: 10.1016/j.jtho.2023.06.010.
- 3 Rudin C M, Brambilla E, Faivre-Finn C and Sage J, Small-cell lung cancer, *Nat Rev Dis Primers*, 2021, **7**(1), 3, doi: 10.1038/s41572-020-00235-0.
- 4 Saller J J and Boyle T A, Molecular pathology of lung cancer, *Cold Spring Harb Perspect Med*, 2022, **12**(3), a037812, doi: 10.1101/cshperspect.a037812.
- 5 Pérez-Ramírez C, Canãdas-Garre M, Molina M Á, Faus-Dáder M J and Calleja-Hernández M Á, PTEN and PI3K/AKT in non-small-cell lung cancer, *Pharmacogenomics*, 2015, **16**(16), 1843–1862, doi: 10.2217/pgs.15.122.
- 6 Jonna S, Reuss J E, Kim C and Liu S V, Oral Chemotherapy for treatment of lung cancer, *Front Oncol*, 2020, **10**, doi: 10.3389/fonc.2020.00793.
- 7 Nashira P D, Wisanti and Putri E K, Character markers of rambutan (*Nephelium lappaceum* L.) varieties based on morphological characters, *Lentera Bio*, 2022, **11**(2), 247–254, doi: 10.26740/lenterabio.v11n2.p247-254.

- 8 Lee Y R, Cho H M, Park E J, Zhang M, Doan T P, *et al.*, Metabolite profiling of rambutan (*Nephelium lappaceum* L.) seeds using uplc-qtofms/ms and senomorphic effects in aged human dermal fibroblasts, *Nutrients*, 2020, **12**(15), 1430, doi: 10.3390/nu12051430.
- 9 Perumal A, AlSalhi M S, Kanakarajan S, Devanesan S, Selvaraj R, *et al.*, Phytochemical evaluation and anticancer activity of rambutan (*Nephelium lappaceum*) fruit endocarp extracts against human hepatocellular carcinoma (HepG-2) cells, *Saudi J Biol Sci*, 2021, **28**(3), 1816–1825, doi: 10.1016/j.sjbs.2020.12.027.
- 10 Hernández-Hernández C, Aguilar C N, Rodríguez-Herrera R, Flores-Gallegos A C, Morlett-Chávez J, *et al.*, Rambutan (*Nephelium lappaceum* L.): Nutritional and functional properties, *Trends Food Sci Technol*, 2019, **85**, 201–210, doi: 10.1016/j.tifs.2019.01.018.
- 11 Utami D, Farid M and Putri R G P, Network pharmacology and molecular docking analysis of *Nephelium lappaceum* (Rambutan) compounds as potential alternative treatments for lung cancer, *Makara J Sci*, 2025, **29**(3), 439–450, doi: 10.7454/mss.v29i3.2712.
- 12 Moradi M, Golmohammadi R, Najafi A, Moosazadeh M M, Fasihi-Ramandi M, *et al.*, A contemporary review on the important role of in silico approaches for managing different aspects of COVID-19 crisis, *Inform Med Unlocked*, 2022, **28**, 100862, doi: 10.1016/j.imu.2022.100862.
- 13 Flores-Holguín N, Frau J and Glossman-Mitnik D, Computational pharmacokinetics report, ADMET study and conceptual DFT-Based estimation of the chemical reactivity properties of marine cyclopeptides, *Chem Open*, 2021, **10**(11), 1142–1149, doi: 10.1002/open.202100178.
- 14 Kim T H, Yu G R, Kim H, Kim J E, Lim D W, *et al.*, Network pharmacological analysis of a new herbal combination targeting hyperlipidemia and efficacy validation *In vitro*, *Curr Issues Mol Biol*, 2023, **45**(2), 1314–1332, doi: 10.3390/cimb45020086.
- 15 Agu P C, Afiukwa C A, Orji O U, Ezech E M, Ofoke I H, *et al.*, Molecular docking as a tool for the discovery of molecular targets of nutraceuticals in diseases management, *Sci Rep*, 2023, **13**(1), 13398, doi: 10.1038/s41598-023-40160-2.
- 16 Yang C, Chen E A and Zhang Y, Protein–Ligand docking in the machine-learning era, *Molecules*, 2022, **27**(14), 4568, doi: 10.3390/molecules27144568.
- 17 Abdul-Hammed M, Adedotun I O, Olajide M, Irabor C O, Afolabi T I, *et al.*, Virtual screening, ADMET profiling, PASS prediction, and bioactivity studies of potential inhibitory roles of alkaloids, phytosterols, and flavonoids against COVID-19 main protease (Mpro), *Nat Prod Res*, 2022, **36**(12), 3110–3116, doi: 10.1080/14786419.2021.1935933.
- 18 Bultum L E, Tolossa G B, Kim G, Kwon O and Lee D, *In silico* activity and ADMET profiling of phytochemicals from Ethiopian indigenous aloes using pharmacophore models, *Sci Rep*, 2022, **12**, doi: 10.1038/s41598-022-26446-x.
- 19 Ramírez D and Caballero J, Is it reliable to take the molecular docking top scoring position as the best solution without considering available structural data?, *Molecules*, 2018, **23**(5), doi: 10.3390/molecules23051038.
- 20 Lena N, Jamil A S, Muchlisin M A and Almutahrihan I F, Pharmacological network analysis of guava (*Guazuma ulmifolia* Lamk.) as an immunomodulator, *J Islamic Pharm*, 2023, **8**(2), 1–6.
- 21 Aleksander S A, Balhoff J, Carbon S, Cherry J M, Drabkin H J, *et al.*, The gene ontology knowledgebase in 2023, *Genetics*, 2023, **224**(1), doi: 10.1093/genetics/iyad031.
- 22 Amata I, Maffei M and Pons M, Phosphorylation of unique domains of Src family kinases, *Front Genet*, 2014, **5**, doi: 10.3389/fgene.2014.00181.
- 23 Ngan E, Stoletov K, Smith H W, Common J, Muller W J, *et al.*, LPP is a Src substrate required for invadopodia formation & efficient breast cancer lung metastasis, *Nat Commun*, 2017, **8**, doi: 10.1038/ncomms15059.
- 24 Martellucci S, Clementi L, Sabetta S, Mattei V, Botta L, *et al.*, Src family kinases as therapeutic targets in advanced solid tumors: What we have learned so far, *Cancers (Basel)*, 2020, **12**(6), doi: 10.3390/cancers12061448.
- 25 Lai Y H, Lin S Y, Wu Y S, Chen H W and Chen J J W, AC-93253 iodide, a novel Src inhibitor, suppresses NSCLC progression by modulating multiple Src-related signaling pathways, *J Hematol Oncol*, 2017, **10**(1), doi: 10.1186/s13045-017-0539-3.
- 26 Belli S, Esposito D, Servetto A, Pesapane A, Formisano L, *et al.*, C-Src and EGFR inhibition in molecular cancer therapy: What else can we improve?, *Cancers (Basel)*, 2020, **12**(6), 1–16, doi: 10.3390/cancers12061489.
- 27 Zhong W, Yang X, Yan H, Zhang X, Su J, *et al.*, Phase II study of biomarker-guided neoadjuvant treatment strategy for IIIA-N2 non-small cell lung cancer based on epidermal growth factor receptor mutation status, *J Hematol Oncol*, 2015, **8**(54), doi: 10.1186/s13045-015-0151-3.
- 28 Pecci F, Cantini L, Metro G, Ricciuti B, Lamberti G, *et al.*, Non-small-cell lung cancer: how to manage EGFR-mutated disease, *Drugs Context*, 2022, **11**, doi: 10.7573/dic.2022-4-1.
- 29 Kobayashi Y and Mitsudomi T, Not all epidermal growth factor receptor mutations in lung cancer are created equal: Perspectives for individualised treatment strategy, *Cancer Sci*, 2016, **107**(9), 1179–1186, doi: 10.1111/cas.12996.
- 30 O'Leary C, Gasper H, Sahin K B, Tang M, Kulasinghe A, *et al.*, Epidermal growth factor receptor (EGFR)-mutated non-small-cell lung cancer (NSCLC), *Pharmaceuticals*, 2020, **13**(10), 1–16, doi: 10.3390/ph13100273.
- 31 Farid M, Rastrani A, Rahma A A and Ramadhania W A, Prediction of *Artocarpus altilis* potential as an anti breast cancer by inhibiting EGFR: A molecular docking study, *Biol Med Nat Prod Chem*, 2025, **14**(1), 199–204, doi: 10.14421/biomedich.2025.141.199-204.
- 32 Tsong J L, Goh L P W, Gansau J A and How S E, Review of *nephelium lappaceum* and *nephelium ramboutan-ake*: A high potential supplement, *Molecules*, 2021, **26**(22), doi: 10.3390/molecules26227005.
- 33 Zhou Z, Tang M, Liu Y, Zhang Z, Lu R, *et al.*, Apigenin inhibits cell proliferation, migration, and invasion by targeting Akt in the A549 human lung cancer cell line, *Anticancer Drugs*, 2017, **28**(4), 446–456, doi: 10.1097/CAD.0000000000000479.
- 34 Lee Y M, Lee G, Oh T I, Kim B M, Shim D W, *et al.*, Inhibition of glutamine utilisation sensitises lung cancer cells to apigenin-induced apoptosis resulting from metabolic and oxidative stress, *Int J Oncol*, 2016, **48**(1), 399–408, doi: 10.3892/ijo.2015.3243.